行政院國家科學委員會專題研究計畫 成果報告

碎形分析法應用在不同呼吸形態下對植物人自律神經功能之評估

研究成果報告(精簡版)

計 畫 類 別 ：個別型
計 畫 編 號 ：NSC 94-2320-B-038-017-
執 行 期 間 ：94 年 08 月 01 日至 96 年 07 月 31 日
執 行 單 位 ：臺北醫學大學通識教育中心

計 畫 主 持 人：潘力誠
共 同 主 持 人：邊苗瑛、林伯威
計畫參與人員： 大學生-兼任助理：吳宗臨、林雅婷、胡家豪、李均浩

處 理 方 式 ：本計畫可公開查詢

中 華 民 國 96 年 10 月 30 日

附件一

行政院國家科學委員會補助專題研究計畫 ■ 成 果 報 告 □期中進度報告

碎形分析法應用在不同呼吸形態下對植物人自律神經功能之評估

計畫類別：■ 個別型計畫　　□ 整合型計畫
計畫編號：NSC 94－2320－B －038 －017－
執行期間：　94 年　8 月　1 日至　96 年 7 月 31 日

計畫主持人：潘力誠

共同主持人：邊苗瑛、林伯威

計畫參與人員： 吳宗臨、林雅婷、胡家豪、李均浩

成果報告類型(依經費核定清單規定繳交)：■精簡報告　□完整報告

本成果報告包括以下應繳交之附件：
□赴國外出差或研習心得報告一份
□赴大陸地區出差或研習心得報告一份
□出席國際學術會議心得報告及發表之論文各一份
□國際合作研究計畫國外研究報告書一份

處理方式：除產學合作研究計畫、提升產業技術及人才培育研究計畫、列管計畫及下列情形者外，得立即公開查詢
□涉及專利或其他智慧財產權，□一年□二年後可公開查詢

執行單位：台北醫學大學 通識教育中心

中　華　民　國　96 年　10 月　30 日

Introduction

Data that obtained from observation of a phenomenon over time are extremely common in biological sciences. We observe the electrical activity of the heart at millisecond intervals. The fluctuations in mammalian blood flow and pressures. The oscillation of the intratubular pressure in rats. The list of areas in which time series are observed and analyzed is plenty. In general, the purpose of time series analysis are two-fold: to understand or model the mechanism that gives rise to an observed pattern and to predict or estimate future values of a series based on the pass history of that series. (Bassingthwaighte et al. 1994; Kaplan and Glass 1995; Abarbanel 1996; Kantz and Schreiber 1997; Mandelbrot 1999; West 1999; Bunde et al. 2002; Doukhan et al. 2003)

In Fractals, the numerical categorization of the complexity of a fractal process has been developed by Mandelbrot (1967). He introduced the concept of the fractal dimension. Since then fractal dimension has been used to described numerous complicated phenomenon: the paths of finely divided particles in a suspension of continuous medium (Brownian motion), growth paths of cells, the structure of coast lines, snow flakes, branching bronchial tree, the fluctuation over time in human blood flows and pressure, ictal electroencephalograph signals, sinus electrical rhythm. Nevertheless, it is still in the stage susceptible to transformation, and its ultimate importance as an investigative tool in physiology is not fully established (Butler et al, 1994).

For example, the accuracy of the measured contour length of a fractal line improves as the measuring stick gets smaller. The best estimate of dimension (D) therefore should be determined from the measurements obtained using the smaller measurement segments. Since in most circumstances the optimal length of subdivision of the measuring stick is not known, the use of longer data segments it is often suggested (Camastra, et al, 2002).

Furthermore in a real system, there will be measurement errors, and these errors will become more important as the scale of measuring device decreases. In addition, depending on the noise characteristics, as the scale of measuring device becomes smaller, the effect of the random noise superimposed on a fractal signal will also become obvious. Katz & George (1985, 1987) showed that the estimated Fractal dimension for a population of cell growth paths was approximately lognormally-distributed. Standard statistics could be done on the logarithms of the Hurst coefficient [log (D)]. With this measure, trails of biological movement in two-dimensional plan can be analyzed to determine the likelihood before and after experimental interventions. However, due the differences in the nature of fractal process such measure has not yet being applied to observations made over time.

The beat-to-beat variation in the heart rate of humans is generated by a complex process and displays inhomogeneous, nonstationary extremely irregular temporal organization. (Golodberger et al. 1985, 1992) The physiological mechanisms of cardiac control expected to result from both intrinsic and extrinsic factors operating at different time scales or resolution have not been identified clearly.(Meyer M 2003) Studies have showed that the complex dynamics of the cardiac rhythm could be resulted from an autonomous low-dimensional deterministically chaotic system (Lefebvre et al. 1993;Yamamoto et al. 1993; Kanters et al. 1994; Sugihara et al. 1996; Poon and Merrill 1997). Heart rate is high-dimensional and its variability often modified by

variables such as autonomic outflow, respiration, arterial blood gases sensory feedback, and various hormones. For any deterministic systems the entire system's dynamics may be describe by a single systemic variable, however the feasibility of this approach for noisy biological time series has not been fully studied.

Persistent vegetative state (PVS) resulting from traumatic or non-traumatic brain injuries is a state of eyes-open unconsciousness with sleep–wake cycles in which the patients are incapable of awareness of themselves or their environment for at least 1 month (The Multi-Society Task Force on PVS, 1994; Zeman, 1997). Due to damage to the cerebral hemispheres, PVS patients show no evidence of sustained, reproducible, purposeful, or voluntary behavior responses to visual, auditory, tactile, or noxious stimuli, and also show no language comprehension or expression (The Multi-Society Task Force on PVS, 1994). Because PVS patients have complete or partial preservation of the hypothalamic and brainstem autonomic functions, they have spontaneous respiration (The Multi-Society Task Force on PVS, 1994; Zeman, 1997).

Study Purpose

Current study proposes a novel dimension estimation process, based on spectral analysis for short-period fractal time series. A moving window technique, along weighted moving average optimized with least mean square algorithm, will be implemented for the estimation of fractal exponent. Particular effort is addressed in the accelerated convergent effects of weighted moving average and that of least mean square algorithm for selection of proper signal length for without compromise on prediction power for minimum step change in signal complexity.

In addition to the surrogate data, we also test the clinical feasibility of this proposed method. Points of interest will include: (1) to analyze the spontaneous breathing patterns of PVS patients and normal control volunteers, (2) to assess the effects of inhalation of 100% O_2 on their respiratory instability, (4) to apply the proposed method on RR-interval from ECG data within PVS group and between PVS and normal control ones for the assessment of their corresponding autonomic function. Comparison will also be performed in linear and nonlinear aspects of the time series, as well as between cardiac and respiratory autonomic influence for PVS.

Reference

1. Abarbanel HDI (1996) Analysis of observed chaotic data. Springer-Verlag, Berlin Heidelberg New York
2. Bassingthwaighte JB, Liebovitch LS, West BJ (1994) Fractalphysiology. Oxford University Press, New York
3. Bien,M.Y., Hseu, S.S.,Yien,H.W.,Kuo, B.I.T., Lin,Y.T.,Wang, J.H., Kou, Y.R., 2004. Breathing pattern variability: a weaning predicttor in postoperative patients recovering from systemic inflammatory response syndrome. Intensive Care Med. 30, 241–247.
4. Brack, T., Jubran, A., Tobin, M.J., 2002. Dyspnea and decreased variability of breathing in patients with restrictive lung disease. Am. J. Respir. Crit. Care Med. 165, 1260–1264.
5. Bunde A, Krapp J, Schellnhuber HJ (2002) The science of disasters. Springer-Verlag, Berlin

Heidelberg New York
6. Butler G.., Yamamoto Y., Hughson R. Fractal nature of short-term systolic BP and HR variability during lower body negative pressure. *Am J Physiol.* 267(36), R26-R33, 1994.
7. Doukhan P, Oppenheim G, Taqqu MS (2003) Theory and applications of long-range dependence. Birkha·· user, Basel
8. Golodberger A. L.., West B. J., and Mandell A. J> On a mechanism of cardiac electrical stability. The fractal hypothesis. Biophys. J. 48:525-528, 1985.
9. Goldberger A. L. Fractal mechanisms in the electrophysiology of the heart. *IEEE Engineering in Medicine and Biology* June:47-52, 1992
10. Kanters JK, Holstein-Rathlou NH, Agner E (1994) Lack of evidence for low-dimensional chaos in heart rate variability. J Cardiovasc Electrophysiol 5:591–601
11. Kantz H, Schreiber T (1997) Nonlinear time series analysis.Cambridge University Press, New York
12. Kaplan DT, Glass L (1995) Understanding nonlinear dynamics. Springer-Verlag, Berlin Heidelberg New York
13. Katz M. J., and George E. B. Fractal and the analysis of growth path. *Bull. Math. Biol.* 47:273-286, 1985.
14. Katz M. J. Fractals and the analysis of waveforms. *Biol. Med.* 18:145-156, 1987.
15. Lefebvre JH, Goodings DA, Kamath MV, Fallen EL (1993) Predictability of normal heart rhythms and deterministic chaos. Chaos 3:267–276
16. Leung, R.S.T., Bradley, T.D., 2001. Sleep apnea and cardiovascular disease. Am. J. Respir. Crit. Care Med. 164, 2147–2165.
17. Longobardo, G.S., Cherniack, N.S., Fishman, A.P., 1966. Cheyne–Stokes breathing produced by a model of the human respiratory system. J. Appl. Physiol. 21, 1839–1846
18. Loveridge, B., West, P., Anthonisen, N.R., Kryger, M.H., 1984. Breathing patterns in patients with chronic obstructive pulmonary disease. Am. Rev. Respir. Dis. 130, 730–733.
19. Mandelbrot B. B. How long is the coast of Britain? Satistical self-similarity and fractional dimension. Science 156:636-638, 1967.
20. Mandelbrot BB (1999) Multifractals and 1/f noise. Springer-Verlag, Berlin Heidelberg New York
21. Meyer M Self-affine fractal variability of human heartbeat interval dynamics in health and disease. European Journal of Applied Physiology. 90(3-4):305-16, 2003 Oct.
22. Naughton, M.T., 1998. Pathophysiology and treatment of Cheyne–Stokes respiration. Thorax 53, 514–518.
23. Poon C-S, Merrill CK (1997) Decrease of cardiac chaos in congestive heart failure. Nature 389:492–495
24. Ponikowski, P., Anker, S.D., Chua, T.P., Francis, D., Banasiak, W., Poole-Wilson, P.A., Coats, A.J.S., Piepoli, M., 1999. Oscillatory breathing patterns during wakefulness in patients with chronic heart failure. Circulation 100, 2418–2424.
25. Sugihara G, Allan O, Sobel D, Allan KD (1996) Nonlinear control of heart rate variabil
26. Tobin, M.J., Chadha, T.S., Jenouri, G., Birch, S.J., Gazeroglu, H.B., Sackner, M.A., 1983a. Breathing patterns. 1. Normal subjects. Chest 84, 202–205.
27. Tobin, M.J., Chadha, T.S., Jenouri, G., Birch, S.J., Gazeroglu, H.B., Sackner, M.A., 1983b.

28. Tobin, M.J., Mador, M.J., Guenther, S.M., Lodato, R.F., Sackner, M.A., 1988. Variability of resting respiratory drive
29. Voss RF: Fractals in nature: From characterization to simulation. In: Peitgen HO, Saupe D (Eds) ; Springer-Verlang, New York, pp21-70, 1988.
30. West BJ (1999) Physiology, promiscuity and prophecy at the millennium:a tale of trails. Word Scientific, Singapore
31. Yamamoto Y, Hughson RL, Sutton JR, Houston CS, Cymerman A, Fallen EL, Kamath MV (1993) Operation Everest II: an indicationof deterministic chaos in human heart rate variability at simulated altitude. Biol Cybern 69:205–212
32. Zeman, A., 1997. Persistent vegetative state. Lancet 350, 795–799.

Material and Method

Numerical Simulation on Fractal Analysis:

Current study focuses on the effects of the length of signal and of the introduction of a analysis window on the accuracy of estimate of H. Extension of signal range is implemented with length from 2^5 to 2^{12} numbered time points and with value of dimension from 0.1 to 0.9. Dimension estimates from various window sizes are computed. Optimized weighted window is used for the acceleration convergence of estimates when small analysis widow is used.

Fractal Signal Generation: As reported by Mandelbrot and Wallis, Fractional Brownian motion and its derivative frequently show a broadband 1/f-like power spectrum. Mandelbrot and Wallis presented a simple definition of the Fractal Brownian motion with spectral theory: white noises are all its repeated integrals and derivatives having a spectral density of the form $1/f^{\beta}$, where f is the frequency, and β an integer. Because determining H or D from a fractal Brownian motion is difficult [8,16], the fractional Brownian noise is needed, which is the successive difference between points of an fractional Brownian motion. Fractional Brownian noises are defined as having a spectral density of the same form, with β a non-integer fraction, hence the name fractional (Brownian) nose, $\beta = 2H - 1$. The fractional dimension related to H as $D = E + 1 - H$, where E is the Euclidean dimension. [5].

Signal Synthesis: The Spectrum synthesis method (SSM) will be used in current study to generate fractal signal with known dimension. The SSM synthesis method generates the fractal signal by computing the back-transform of power spectrum described by a power law function:

$$|A|^2 = 1/f^{\beta} \qquad (3\text{-}1)$$

where $|A|$ is the magnitude of the spectral density at frequency f, with an exponent equal to $\beta = 2H + 1$. Given the desired H, with magnitude of the spectral density $|A|$ set to equal a constant for all frequencies, and the phases drawn randomly from a uniform distribution, the time series of the fractional Brownian motion can then be produced by performing the inverse transform of the Fourier spectrum. The imaginary part of the time series is often ignored.

Estimation of Hurst coefficients. The square of the amplitude from the Fourier transform of a pure

fractional Brownian motion is known to follow a power law function. [5] When the logarithm of the amplitude of the individual frequency components of the signals vs. the logarithm of the frequency is plotted for fractal signals, the slope of the relationship between the two components can be a straight line with slope -β [voss, 1988, 39] When the derivative is taken from fractional signals, β is reduced by two. Thus, for fractional Brownian noise, fBn β is expected to be

$$\beta = 2H - 1 \quad \text{.....(3-2)}$$

The fractal dimension relates to H as

$$D = E + 1 - H \quad \text{.....(3-2)}$$

, where E is the Euclidean dimension (Voss et al., 1988)

Since frequency axis was no longer in linear scale in the log-log plot between power spectrum of signals and the frequency, as logarithm of frequency increases density of data points increases. With least-square algorithm, a straight line was fitted through these data points. Fractal dimension was calculated by inserting the slope of the straight line into equation 3-2 and 3-3.

Moving Window Analysis (MMA): Prior to the application of dimension estimation, various sizes of the analysis window (W*a*) will be selected. For each length L of a fractal time series, one analysis windows W$n = 2^i$, i = 5, 6,...., 12, is selected first, the estimation start from first numbered point and advance through the entire length of the data with a overlap of L-4 time points, which yields an estimated sequence, $\hat{h}(1)$, $\hat{h}(2)$, ..., $\hat{h}$(k).

Weighted Moving Average (WMA): Given the a set of weights namely, $w(1)$,$w(2)$, ….,w(n) for the resulting sequence of dimension estimates, $\hat{h}(1)$, $\hat{h}(2)$, ..., $\hat{h}$(k), weighted average is defined by:

$$\hat{H}(k) = \frac{w(n)h(k) + w(n-1)h(k-1) + ...w(1)h(k-n-1)}{w(n) + w(n-1) + ... + w(1)} \quad \text{.....(3-3)}$$

, where n is number of the weight used and k is number of dimension estimates sequence from MMA method. The weighted moving average are computed by shifting a window of size n over a preset overlap distance l, where l < n <k. The mean square error (MSE) is calculated with the formula:

$$MSE = \sum_{j=n+l}^{k} \frac{[h(t) - \hat{H}(t)]}{k-n-l+1} \quad \text{.....(3-4)}$$

Different window size is computed along with its corresponding MSE. Value of n with least value of MSE is choosing for subsequent analysis.

Analysis of Clinical Feasibility : *Subjects:* Thirty PVS patients from three nursing homes will be included in this study as the experimental group. Following criteria are used for the screening the test subjects: (1) unaware of self and environment for at least 12 months due to severe brain damage from various etiologies; (2) completely bedridden, not able to take care of themselves and to communicate with other persons; (3) their Glasgow coma scale (Shah, 1999) was ≤8 and their Barthel Index Score (Mahoney and Barthel, 1965) was <20; (4) had been able to breathe room air on their own through the tracheostomy tube and free form ventilator support 113 for at least 6 months with acceptable blood gases data; (5) clinically and hemodynamically stable, and having no fever and (6) free from heart failure, pulmonary and renal diseases, and signs of increased intracranial pressure or infection. Another 15 age- and sex-matched normal volunteers

are also included as the control group during the same study period and were free from cardiopulmonary, neuromuscular and renal diseases, and without histories of smoking and congestive heart failure. These normal volunteers are instructed regarding the study procedure, but will be blinded to the study design. For all subjects, sedatives, hypnotics and narcotics will be discontinued for at least 8 h prior to the study. Appropriate institutional review board approval will be obtained and written informed consent is obtained from the patient's legal guardian and from the control subjects.

Data analysis: Power spectral analysis of the breath-by-breath data is re-sampled at evenly spaced time intervals of 8ms by a linear interpolation. The mean value of each set of data was subtracted from the time series data to remove the direct current component. A Hanning window in the time domain is used to attenuate the leakage effect. The time series data is appended by zero valued samples to the size of 262144 (218) data points. The resulting power spectra have a theoretic resolution of $4.77\times10-4$ Hz. The graph of the power spectrum will be smoothed by a moving average filter set at a size of 15. The density values of total power and very-low-frequency (VLF) power were calculated as the integral under the power spectral function with a frequency range between 0.001–0.5 Hz (oscillatory cycle duration = 1000–2 s or 0.06–30 cycles/min) and 0.003–0.04 Hz (oscillatory cycle duration = 333–25 s or 0.18–2.4 cycles/min), respectively. The frequency range of VLF power was chosen to cover the possible range of cycle duration of OB reported previously (Bruce and Daubenspeck, 1995; Hall et al., 1996; Khoo, 1999; Ponikowski et al., 1999).

Continuous ECG monitoring and heart rate analysis: Thirty-minutes continuous ECG recordings will be obtained for analysis in all subjects using a holter type deivce (Del Mar FlashCorder Holter Recorder, Model 485) recording standard leads CM1 and CM5. The following time-domain indices were evaluated: standard deviation of all RR intervals, 24 h triangle index, standard deviation of 5-min mean RR intervals and the root mean square of differences of successive RR intervals. Frequency domain (spectral analysis) are undertaken by modified spectral analysis. This process operated on data of 30 min segments of each experiment condition. Time periods where there are excessive movements will be excluded. Spectral plots will also be used to identify the low-frequency (LF) component (0.03 to 0.14 Hz) and the high-frequency (HF) component (0.18 to 0.40 Hz). Indices are expressed in normalized units (n.u.), or the relative percentage compared to the total oscillatory power.

Results and Discussion

Although, dimension estimates from time series generated by SSM has been shown to be Gaussian-like for estimation process such as dispersional analysis. However, to further rule out the possibility for differences when method such as spectral analysis is applied, we've created and tested the data set with 200 fractal time series generated by SSM, each with selection of length N, (N = 32, 64, 128, 256, 51 2,1024, 2048, 4096, 8192), and roughness H, (H = 0.1, 0.2, 0.3, 0.4, 0.5, 0.6, 0.7, 0.8, 0.9). To test for its normality, we've calculated the kurtosis and skewness for these 3600 fractal time series. When lumped together the data from the calculated skewness where input dimensionality is the same but with different signal length are lumped together, the mean calculated skewness level will all be negative and will be slightly lower than

but different not as much as that of the standard level for normal distribution (β_1 = 0). On the other hand, when the calculated kurtosis are subjected to the same lumping process, mean level for the kurtosis are mostly leptokurtic, and are slightly greater than but different not as much as that of the standard level for normal distribution (β_2 = 3). Please see Table 1 for the listing of detailed values for the mean and SD of the lumped kurtosis and skewness at each input complexity level. Therefore, it is proposed that SSM along with spectral analysis can create fractal time series with Gaussian-like estimated dimension distribution, and the normal statistics will be applied in the subsequent study.

With the same range of *H*'s and *N*'s as there is in the test for Gaussian normal distribution, Table 2 lists the mean estimated dimension and its standard deviation for 200 trials via spectral analysis. From the plot between input dimension level and the mean estimated dimension, there is an over-estimation tendency in the range where input dimension level *H*'s is >0.5. It is then being under-estimated in the range where *H*'s is ≤ 0.5. Also, when looking at the each theoretic level and compare it with the corresponding estimated dimension level; the deviation from the theoretic dimensionality is more prominent for signal with shorter data length than that of the longer ones. Standard deviation on the other hand shows a much different profile.

N Points	0.1	0.2	0.3	0.4	0.5	0.6	0.7	0.8	0.9
32	0.1035	0.2004	0.2858	0.4198	0.4891	0.6076	0.7149	0.8284	0.9371
	0.2069	0.2005	0.2122	0.2054	0.2005	0.2110	0.2083	0.1939	0.1976
64	0.0872	0.1838	0.2877	0.4084	0.5071	0.6187	0.7185	0.8214	0.9216
	0.1541	0.1612	0.1504	0.1325	0.1382	0.1438	0.1453	0.1331	0.1324
128	0.0976	0.1944	0.2987	0.4087	0.5128	0.6046	0.7045	0.8081	0.9111
	0.0953	0.1040	0.1002	0.0946	0.1022	0.0974	0.1018	0.0934	0.0946
256	0.0964	0.1936	0.3014	0.4051	0.4928	0.5997	0.7040	0.7988	0.9057
	0.0642	0.0730	0.0695	0.0714	0.0700	0.0764	0.0754	0.0709	0.0710
512	0.1030	0.1958	0.3029	0.3943	0.5027	0.6028	0.7042	0.7980	0.9027
	0.0503	0.0496	0.0524	0.0515	0.0457	0.0451	0.0484	0.0446	0.0504
1024	0.0984	0.2029	0.3018	0.4024	0.5018	0.6027	0.7009	0.7982	0.9074
	0.0357	0.0353	0.0373	0.0341	0.0357	0.0334	0.0337	0.0341	0.0321
2048	0.0982	0.2000	0.2992	0.4015	0.5019	0.6005	0.7004	0.8026	0.9000
	0.0262	0.0241	0.0251	0.0289	0.0240	0.0239	0.0216	0.0241	0.0255
4096	0.0997	0.2023	0.3007	0.4014	0.5012	0.6004	0.7002	0.8018	0.9009
	0.0171	0.0170	0.0169	0.0177	0.0178	0.0179	0.0161	0.0160	0.0174
8192	0.1010	0.1996	0.3010	0.4012	0.4998	0.6011	0.6993	0.8007	0.8997
	0.0114	0.0124	0.0127	0.0110	0.0117	0.0127	0.0120	0.0126	0.0118

The power of the test, defined as the statistical probability that a test will produce a significant difference at a given significant level, is one measure often used to demonstrate the existence of a difference before and after a clinical treatment. However, implementation of such test can work equally well whether the difference that can be detected under a given sample size is the point of interest, or to estimate the sample size required to present a statistical difference between group means is the main focus. With the group and standard error from Table 2, Table 3 presents the model estimated sample sizes required to detect a difference of size ΔH, with 90% power and under 5% significant level for equally sized samples. From this table it is suggested that the sample size required to detect a given difference, say 0.01 in mean of ΔH, will decrease from more 7000 in number with data of length 32 points, and goes down to 25 as data length increases up to 8192 points. Meanwhile, for the same data length, say 128 points, the sample size required to detect a difference with the same statistical power in group mean will decrease from 1575 in number, and goes down to 25 in number as the difference of ΔH increase from 0.01 to 0.08. However, no appreciable difference in the required

Table 3: Sample size required in each group to detect a difference between two means at the 5% significant level with power 90%, using equally sized sample

H=0.3

ΔH \ N	32	64	128	256	512	1024	2048	4096	8192
0.01	7066	3549	1575	757	432	218	99	45	25
0.02	1767	887	394	189	108	55	25	11	6
0.03	785	394	175	84	48	24	11	5	3
0.04	442	222	98	47	27	14	6	3	2
0.05	283	142	63	30	17	9	4	2	1
0.06	196	99	44	21	12	6	3	1	1
0.07	144	72	32	15	9	4	2	1	1
0.08	110	55	25	12	7	3	2	1	0
0.09	87	44	19	9	5	3	1	1	0

H=0.7

ΔH \ N	32	64	128	256	512	1024	2048	4096	8192
0.01	7066	3549	1575	757	432	218	99	45	25
0.02	1767	887	394	189	108	55	25	11	6
0.03	785	394	175	84	48	24	11	5	3
0.04	442	222	98	47	27	14	6	3	2
0.05	283	142	63	30	17	9	4	2	1
0.06	196	99	44	21	12	6	3	1	1
0.07	144	72	32	15	9	4	2	1	1
0.08	110	55	25	12	7	3	2	1	0

sample sizes for the sample power and significant level is observed between dimension estimates from input fractal time series with negative near-neighbor correlation and that with the one which possesses positive near-neighbor correlation.

The use of moving windows with overlaps serves two purposes in current study; one is to increase the sampling number while maintaining the temporal correlation between successive time windows, and the others are to detect transient changes occurred not in mean signal level or absolute amplitude, but in signal complexity. Attached figure plots the mean dimension estimates and its associated error bar over the indicated data size in log of 2 with theoretic input dimension H = 0.75 (or D = 1.25), from 200 trials in each data length (top trace), and from the result of applying a moving window across fractal signal with 8192 points (bottom trace). As is expected, when smaller data length is used, reduction in frequency resolution will cause bias in power density estimate, which is shown here in both cases as the elevated mean and *SD*. However, when the moving widow process is taking less than 256 points out from a total of 8192 points (or 6.25%) in figure 7(b), mean estimated dimension will continue to increase and goes up to twice the input level as bin size decreases further down to 32 points, whereas only small oscillatory changes are observed in mean estimated level for normal sequence.

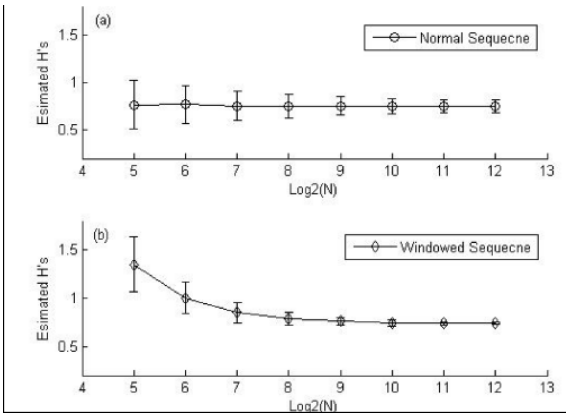

To validate for the proposed method, two fractal time series were created from SSM with step difference in signal complexity each with 8192 time points. The first half of the surrogated sequence is with dimension H = 0.6 and is also referred to as the low dimension sequence (LDS), and the second half is with dimension H = 0.7 and is referred to as the high dimension sequence (HDS). Both are adjusted to have zero mean and then connected in succession from LDS to HDS. Prior to the wavelet based analysis, dimension of the combined data series is being calculated via the application of moving window with bin size from 16 points to 4096 points in power of 2, with sift-in distance equal to 4 time points for all window sizes. Wavelet decomposition set at eleventh wavelet scales is then performed, with the DWT algorithm implemented using the Daubechies compactly supported othonormal wavelet transform method of order one. At last, the identification of time location of the joint *fBn* signal is done by reconstruction using the IDWT algorithm only from the 11^{th} scales of the approximated coefficients of the wavelet decomposed dimension sequence. In addition, the effect of the addition of a Gaussian white noise with signal-to-noise ratio from -20 dB ~ 30 dB is also being tested.

Right figure shows the time evolution for the moving window predicted (in solid line) versus the wavelet modified (in dished line) dimension estimates for a joint time series created with SSM and each with 8192 time points. Although transition from LDS to HDS is observed for the moving window predicted sequence near time location $k \geqq 8000$, however, due to its relatively high local fluctuation, identification of the exact step location

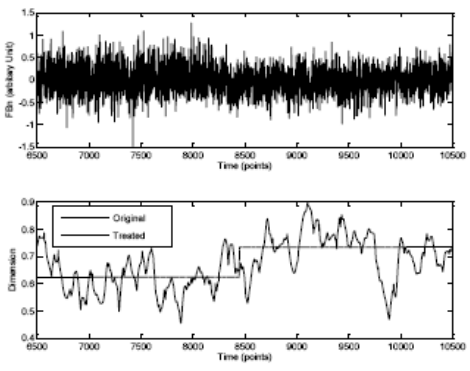

is compromised. One the hand, wavelet predicted dimension sequence shows a clear step-like profile, from which the level of LDS and HDS, the step location and its co responding change in signal complexity can be calculated.

It is observed that smaller analysis window predicts better with less difference between the model-predicted step position and the exact time location. Moreover, this difference is equals to its corresponding bin size of the applied analysis window. This implies that although lager window do perform better in dimension estimation with less variability if moving window technique alone is the used for the dimension estimation, but will add more delay to the predicted step position when further combined with wavelet transform. Moreover, even if all wavelet predicted level for LDS and HDS are higher than the input level, the predicted error calculated from the difference between LDS and HDS decreases as window size increases, and will cross over from positive (over-estimated) to negative (under-estimated) at bin size greater or equal to 1024 points.

Attached figure shows the effect of adding a Gaussian random noise to the wavelet predicted dimension for LDS and HDS at various SNR level. It is noted that there is no appreciable difference between estimated LDS (circle) to HDS (diamond) level until the noise level reaches -15 dB or more. Although the difference between the predicted LDS and HDS dose increases as SNR level increases from -10dB and up, however, the SNR has to reach 10 dB or more before the predicted difference in complexity level become reasonable close with error that is 10% or less to the theoretic level. On the other end of the spectrum, when noise level is at -20dB or less, the test series is completely corrupted and the signal is therefore biased toward random noise.

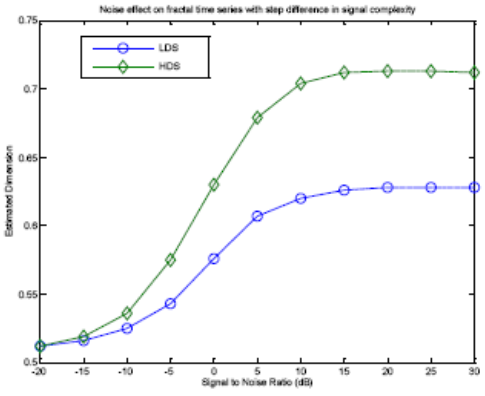

The physical and clinical characteristics of the experimental groups are listed in the following table. As shown, PVS-OB** group had a significantly higher baseline systolic and diastolic blood pressure and a significantly lower *P*ETCO2, as compared to the control group; these three parameters in the PVS-OB** group did not differ from those in the PVS-IB** group. Other characteristics did not vary among the three study groups.

Physical and clinical characteristics of the three study groups

Study groups	Control (n = 15)	PVS-IB (n = 15)	PVS-OB (n = 12)
Age (years)	61.27 ± 12.56	57.27 ± 15.59	69.25 ± 15.10
Sex (male/female)	8/7	9/6	7/5
BMI (kg/m^2)	22.64 ± 3.08	22.37 ± 2.74	21.95 ± 2.80
Vegetative duration (months)	–	82.60 ± 61.73	74.33 ± 36.13
Glasgow coma scale	Clear	7.33 ± 0.72	7.17 ± 0.83
Tracheostomy tube ID	–	7.13 ± 0.55	7.42 ± 0.90
Systolic blood pressure (mmHg)	116.67 ± 11.57	122.00 ± 21.34	130.17 ± 18.55*
Diastolic blood pressure (mmHg)	69.20 ± 8.27	75.77 ± 13.44	79.33 ± 10.66*
Pulse rate (min^{-1})	71.80 ± 9.36	79.21 ± 11.35	80.84 ± 13.47
Oxygen saturation (%)	96.59 ± 1.39	96.31 ± 1.07	95.32 ± 1.63
End-tidal CO_2 (Torr)	43.13 ± 3.38	39.99 ± 4.38	37.20 ± 5.22*

**Persistent vegetative state (PVS), irregular (IB) and oscillatory breathing (OB) represent breathing patterns with increases in non-periodic and periodic variations, respectively, as a manifestation of respiratory instability

For the analysis of autonomic control, we used a decomposition algorithm based on the DWT

where the R-R intervals from ECG were first re-sampled at 2 Hz by a cubic spline interpolation, then, decomposed into six wavelet scales with the sampling period set at 2 second. This resulted in the following set of bandlimits for the filter bank:0.6957, 0.3478, 0.1739, 0.0870, 0.0435, and 0.0217Hz. The DWT algorithm was implemented using the Daubechies compactly supported orthonormal wavelet transform method, with an order of12. Noted also that to decompose the cardiovascular fluctuations, three frequency bands were used which include; the very low-frequency (VLF, centered near 0.04 Hz), low-frequency (LF, near 0.10 Hz) which is effected both by sympathetic and parasympathetic activity, and high-frequency (HF, above 0.15 Hz) that is associated with parasympathetic activity. Wavelet decomposition of the RR variability signal from representative subject is shown in the bottom left figure. Vertical from top to bottom, x(n) represents the original RR intervals, approximated composition at scale 6 (J = 6) , and detailed composition at scale 6 and followed by detailed composition from scale 5 to scale 1. , as well as instantaneous power estimates for the VLF, LF, and HF components of the RR variability signal for the same subject (bottom right).